*The British Journal of Radiology, 84* (2011), e65–e67

CASE REPORT

# FDG-PET/CT-guided biopsy of bone metastases sets a new course in patient management after extensive imaging and multiple futile biopsies

[1]M K WERNER, MD, [1]P ASCHOFF, MD, [2]M REIMOLD, MD and [1]C PFANNENBERG, MD

[1]*Department of Diagnostic and Interventional Radiology, and* [2]*Department of Nuclear Medicine, Eberhard-Karls-University Medical Center, Tübingen, Germany*

**ABSTRACT.** A 73-year-old man with a history of prostate and bladder carcinoma and persistent back pain was diagnosed by MRI with multiple vertebral metastases including a compression fracture of T7. He received radiotherapy for pain relief and for vertebral instability with incipient spinal stenosis, but additional targeted systemic therapy was intended. Therefore, multiple attempts at minimally invasive and open biopsies for histological characterisation of the bone metastases were performed, but failed to provide a conclusive specimen, although CT, MRI and bone scintigraphy were used for biopsy planning. Only histopathological analysis of an $^{18}$F-fluorodeoxyglucose-positron emission tomography (FDG-PET)/CT-guided additional biopsy at a site with high metabolic activity yielded the final diagnosis of bone metastases of a neuroendocrine small cell cancer of unknown origin; hence, the patient had a third malignancy requiring a different therapy regimen and diagnostic work-up.

Received 9 March 2010
Accepted 7 April 2010

DOI: 10.1259/bjr/26998246



Different imaging modalities are conjointly used for the appropriate diagnosis and staging of cancer patients [1–3]. The combined evaluation of CT, MRI and positron emission tomography (PET) yields a substantial increase in sensitivity for the detection of various malignancies [4, 5], although pathological analysis remains the gold standard for further characterisation in order to provide specific, targeted therapy. Dual-modality PET/CT with $^{18}$F-fluorodeoxyglucose (FDG) plays an increasing role in oncological imaging [6, 7]. One reason is that metabolic activity, reflected by FDG uptake, may allow viable tumour and post-treatment changes to be differentiated [8]. Here, we present a case in which FDG-PET/CT finally led to a successful biopsy and diagnosis of a third malignancy, whereas multiple MRI- and CT-guided biopsies had failed to provide a conclusive specimen.

## Case report

A 73-year-old man with persistent and increasing back pain was diagnosed with multiple bone metastases by an outpatient MRI showing multiple hyperintense lesions in $T_2$ weighted sequences in the vertebral column, including a compression fracture of T7 (Figure 1a,b). Because of pain and the pathological fracture of T7 posing a risk of spinal cord compression, the patient was treated with immediate outpatient radiation therapy of the thoracic and lumbar spine. The patient had a medical history of prostatic adenocarcinoma (pT2a pN0 G2, Gleason score 4) treated with radical prostatectomy 4 years previously (pre-operative PSA (prostate specific antigen), 2.1 ng ml$^{-1}$; current PSA, below detection limit) and invasive urothelial bladder carcinoma (pT1 pN0 (0/15) pR0 G3) treated with total cystectomy 5 months previously. Follow-up CT and technetium-99m–diphosphonate ($^{99m}$Tc-DPD) bone scintigraphy 4 months earlier showed no abnormalities.

After radiotherapy, the patient was hospitalised for further staging. In order to determine the appropriate therapy regimen (according to current guidelines [9, 10]), it was important to find out to which primary tumour the bone metastases were to be attributed. If the patient's prostate carcinoma had spread to the skeleton, radiation and anti-hormonal therapy, potentially later escalated with docetaxel chemotherapy, would have been the therapy of choice. If the patient's urothelial bladder carcinoma had been the cause of metastatic bone disease, therapy would have been initiated with gemcitabine and cisplatin.

An additional MRI scan of the spine (Figure 1c) and whole-body CT (Figure 1d,e) both confirmed multiple vertebral metastases, and a transpedicular biopsy of T7 and S1 was performed in order to determine the origin of the metastases and to initiate adequate treatment, yet without a conclusive specimen: no malignant cells were contained in the specimen, only normal and partially necrotic haematopoietic cells and trabecular bone. The amount of tissue was considered sufficient.

Address correspondence to: Matthias K Werner, MD, Eberhard-Karls-University Medical Center, Department of Diagnostic and Interventional Radiology, Hoppe-Seyler-Str. 3, 72076 Tübingen, Germany. E-mail: Matthias.Werner@med.uni-tuebingen.de

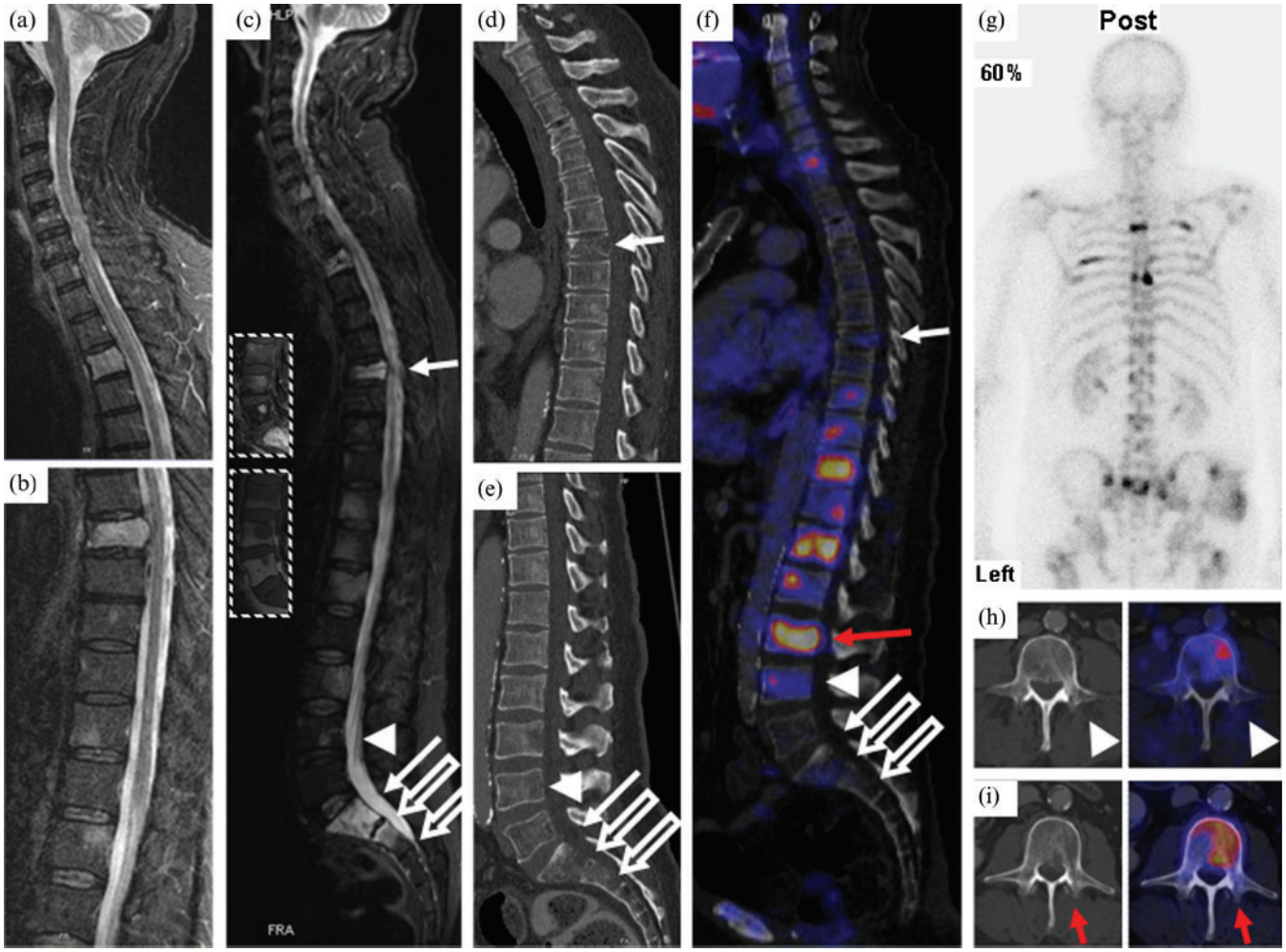


**Figure 1.** (a,b) Outpatient MRI of the spine ($T_2$ weighted turbo inversion recovery magnitude (TIRM) FS) showing vertebrae C1–T5 (a) and T6–L2 (b) prior to radiation therapy. Multiple hyperintense lesions representing vertebral metastases to T3, T7, T11–12, L1, L3, S1–2 and a compression fracture of T7 protruding into the spinal canal are visible. (c) MRI of the spine after radiotherapy ($T_2$ weighted TIRM fat-saturation (FS); insets, $T_1$ weighted turbo spin-echo (TSE) with gadolinium intravenous contrast (top) and $T_1$ weighted TSE (bottom) of L3–S1). Hyperintense lesions appear unchanged in radiated regions. (d,e) Sagittal CT of the thoracic (d) and lumbar (e) spine showing the compression fracture of T7 and inhomogeneous bone structure but no apparent osteolysis. (f) Positron emission tomography (PET)/CT fusion image of the vertebral column with previous biopsy sites (solid arrows, transpedicular biopsy of vertebrae T7 and S1; open arrows, surgical (open) biopsy of vertebral bodies S1 and S2; arrow heads, transpedicular biopsy of vertebra L4) and biopsy site chosen according to PET/CT (red arrow). (g) Bone scintigraphy showing increased uptake of $^{99m}$Tc-DPD in several ribs on the left and right hemithorax, as well as in the vertebral column. (h) PET/CT fusion image of L4: the biopsy channel is visible adjacent to FDG-avid, potentially vital malignant tissue. (i) Retrospective fusion of PET data (right) with post-biopsy CT (left) after PET/CT-planned biopsy of vertebra L3.

Staging was completed with $^{99m}$Tc-DPD bone scintigraphy (Figure 1g), now showing tracer uptake in the S1 and S2 vertebrae, T4, T7–8 and several ribs. A second open biopsy was performed on S1 and S2; however, no malignant tissue was found in the biopsy specimen. A further left transpedicular biopsy of L4 was performed, again without evidence of malignancy.

Because of the therapeutic consequences depending on the descent of the patient's bone metastases, with two different carcinomas in the patient's history, and with different chemotherapy regimens and treatment options pending, histological assessment was considered mandatory and the patient was scheduled for FDG-PET/CT for further biopsy planning. PET/CT showed multiple bone lesions with increased FDG uptake, *e.g.* in the proximal right humerus, the lateral left clavicle, both scapulae, several ribs, several vertebral bodies (most prominent in C7 and T9–L3), the left acetabulum and both proximal femoral bones (Figure 1f). FDG uptake was intense in all lesions outside the irradiated field with a maximum standardised uptake value (SUV) of 14.1 and a minimum SUV of 2.5. In addition, focal FDG uptake could be detected in a liver lesion (segment IV) and in an enlarged inguinal lymph node on the left side.

The sites of previous biopsies (T7, S1, S2) in the irradiated thoracic and lumbar spine showed only faint or absent FDG uptake (Figure 1f). Although some FDG uptake could be observed in L4, the PET/CT fusion showed the biopsy channel from the previous biopsy just lateral to an FDG-avid area (Figure 1h).

Because of its high glucose consumption, the lesion in L3 was selected for subsequent biopsy (red arrow in

Figure 1f,i). Retrospective fusion of post-biopsy CT and pre-biopsy PET data showed the biopsy channel traversing a FDG-avid area within the marrow of L3 (Figure 1i).

Now, from the specimen taken, pathology revealed a small cell carcinoma, not related to the known carcinomas of the prostate and bladder, as indicated by immunohistochemistry: expression of synaptophysin but no expression of the epithelial markers AE1/AE3, cytokeratin 7, the leukocyte marker CD45, CD20, chromogranin A or TTF-1. Tumour cells showed a high proliferation rate (MIB-1 80–90%) and plasma neuron-specific enolase (NSE) was high (423 $\mu g\ l^{-1}$) in the patient. In summary, although small cell carcinomas of the prostate gland as well as the bladder have been reported in the literature [11, 12], histological findings were not compatible with either of the tumour entities known from the medical history of our patient, leading to the diagnosis of a tertiary carcinoma that was a metastatic neuroendocrine small cell cancer of unknown primary. A rare alternative explanation besides a third malignancy as the origin of our patient's metastases could also be small cell components or a divergent clone of either the prostate or urothelial bladder carcinoma that was previously undetected. However, in all three of these possibilities, the adapted chemotherapy regimen would be the same. Therefore, the patient received four cycles of carboplatin/etoposide chemotherapy with a significant reduction in the NSE tumour marker to 8 $\mu g\ l^{-1}$, and after the first cycle the patient had already gone into remission. To date, the patient is alive and is well.

## Discussion

Obtaining tissue samples for further pathological characterisation and the definition of the primary tumour and origin of metastases is part of almost every cancer patient's work-up. Only with a thorough histology-proven diagnosis can targeted and guideline-based therapy be initiated for the benefit of the individual patient.

However, after treatment with radiation or chemotherapy, it can be difficult to distinguish residual tumour from post-radiation changes using morphological imaging modalities [13]. Also, bone scintigraphy as a functional imaging method shows only bone metabolism, not malignancy, and hence may not be specific enough to separate bone remodelling and healing fractures, which are common after treatment of bone metastases [8] from live tumour cells.

Our patient had metastases to the bone marrow and trabecular bone with only minor changes visible on CT and without substantial osteolysis. Therefore, CT and bone scintigraphy were not able to reliably detect malignant bone marrow infiltration. MRI showed malignant bone marrow infiltration as well as post-radiation changes in our patient, yet they were indistinguishable by the MR sequences in our standard protocol.

In contrast, FDG-PET/CT is able to pinpoint areas with increased metabolic activity, and, therefore, directly visualises vital tumour and can offer an important additional benefit for biopsy planning [14] in addition to being a thorough diagnostic tool.

## Conclusion

This case shows how anatomical and functional imaging modalities complement each other to detect malignant bone and bone marrow abnormalities.

## References


1. Lardinois D, Weder W, Hany TF, Kamel EM, Korom S, Seifert B, et al. Staging of non-small-cell lung cancer with integrated positron-emission tomography and computed tomography. N Engl J Med 2003;348:2500–7.
2. Herbertson RA, Lee ST, Tebbutt N, Scott AM. The expanding role of PET technology in the management of patients with colorectal cancer. Ann Oncol 2007;18:1774–81.
3. Piperkova E, Raphael B, Altinyay ME, Castellon I, Libes R, Sandella N, et al. Impact of PET/CT in comparison with same day contrast enhanced CT in breast cancer management. Clin Nucl Med 2007;32:429–34.
4. Margolis DJ, Hoffman JM, Herfkens RJ, Jeffrey RB, Quon A, Gambhir SS. Molecular imaging techniques in body imaging. Radiology 2007;245:333–56.
5. Von Schulthess GK, Hany TF. Imaging and PET-PET/CT imaging. J Radiol 2008;89:438–47.
6. Antoch G, Saoudi N, Kuehl H, Dahmen G, Mueller SP, Beyer T, et al. Accuracy of whole-body dual-modality fluorine-18-2-fluoro-2-deoxy-D-glucose positron emission tomography and computed tomography (FDG-PET/CT) for tumor staging in solid tumors: comparison with CT and PET. J Clin Oncol 2004;22:4357–68.
7. Townsend DW. Dual-modality imaging: combining anatomy and function. J Nucl Med 2008;49:938–55.
8. Shin DS, Shon OJ, Byun SJ, Choi JH, Chun KA, Cho IH. Differentiation between malignant and benign pathologic fractures with F-18-fluoro-2-deoxy-D-glucose positron emission tomography/computed tomography. Skeletal Radiol 2008;37:415–21.
9. National Comprehensive Cancer Network. NCCN clinical practice guidelines in oncology: prostate cancer, v.1.2010. Available from: http://www.nccn.org/professionals/physician_gls/f_guidelines.asp
10. National Comprehensive Cancer Network. NCCN clinical practice guidelines in oncology: bladder cancer, v.1.2010. Available from: http://www.nccn.org/professionals/physician_gls/f_guidelines.asp
11. Chang JM, Lee HJ, Lee SE, Byun SS, Choe GY, Kim SH, et al. Pictorial review: unusual tumours involving the prostate: radiological-pathological findings. Br J Radiol 2008;81:907–15.
12. Gilligana T, Dreicer R. The atypical urothelial cancer patient: management of bladder cancers of non-transitional cell histology and cancers of the ureters and renal pelvis. Semin Oncol 2007;34:145–53.
13. Dotan ZA. Bone imaging in prostate cancer. Nat Clin Pract Urol 2008;5:434–44.
14. Klaeser B, Mueller MD, Schmid RA, Guevara C, Krause T, Wiskirchen J. PET-CT-guided interventions in the management of FDG-positive lesions in patients suffering from solid malignancies: initial experiences. Eur Radiol 2009;19:1780–5.